Practical lab tool for living cells based on microstereolithography and multiple dynamic holographic optical tweezers

Serge Monneret[*a], Federico Belloni[a,b], Didier Marguet[b]
[a]Institut Fresnel, MOSAIC group, UMR 6133 CNRS, Université Paul Cézanne, Marseille, France.
[b]Centre d'Immunologie de Marseille Luminy, MOSAIC group, UMR 6102 CNRS – U136 INSERM, Université de la Méditerranée, Marseille, France.

ABSTRACT

Recent studies have shown that the cell is mechanically differentiated both spatially and temporally, leading to a regional approach in cell behaviour essays. Most experiments are based on spatially-controlled contacts between microbeads and cells. We here propose an apparatus based on holographic optical tweezers to put on a target cell a two- or three-dimensional custom-built pattern of beads, with respect to the target cell shape, with both temporal and spatial dynamic control of each contact. In order to avoid disturbance or contact from the excess beads with the target cell, we keep the beads under isolated condition, by placing them in a confinement chamber made by microstereolithography. Our system exploits a digital display to project binary images on a photocurable resin surface, and induce space-resolved photopolymerisation reactions, constructing three-dimensional micro structures with complex shapes, including reservoirs for the filling, outlets, and confinement chambers. Combination of microfluidics, holographic optical tweezers and one supplementary single manually steerable optical tweezers leads to several experimental procedures allowing the sequential or parallel deposition of beads onto a target, with both a spatial and temporal control.

Keywords: Optical tweezers, microstereolithography

1. INTRODUCTION

In the past ten years there has been an increasing interest in biochemical analysis of living single cells, showing that a lot of crucial biological events depend on specific molecular recognition at the cell plasma membrane. Moreover, recent studies in cell biology have shown that the cell is mechanically differentiated both spatially and temporally, leading to a regional approach in cell behaviour essays [1]. Hence, membrane dynamics must also be strongly dependant on both the temporal and spatial conditions of its stimulation. As a consequence, it would probably be very interesting to be able to excite individual cells, by controlling the stimulation location, the stimulation timing, and the stimulation duration.

In order to determine the local and/or temporal response to stimuli, and therefore draw a map of cells sensitivity, one convenient way is to use optical tweezers to bind opsonized latex beads on the plasma membrane. Optical tweezers [2] are one of the current methods commonly used in biology laboratories for manipulation of bioparticles like cells or bacteria [3]. They are well adapted to trap latex beads and drive them onto individual cells, in order to probe some of their local membrane properties [4-6]. Temporal effects of cell adhesion on mechanical characteristics of single chondrocytes have also been probed [7]. Calcium imaging combined with a single optical trap enabled the T cell contact requirements and polarity to be investigated at the single-cell level. Variations in antibodies density and beads size were used to determine the spatial requirements and the minimum number of receptors which must be engaged to transmit a positive signal [8]. Motion analysis of surface-adherent particles driven by an optical trap was also used to study surface dynamics on living cells, revealing distinguished regions with respect to adhesion, and with respect to particle motion over the path of the bead from the cell edge to the perinuclear area [9].

Mapping the cell sensitivity with multiple optical traps could improve the efficiency of the measurements, but also their versatility. As examples, co-stimulation or serial stimulations of cells could be applied, and could influence the cell behaviour. Therefore, we propose to achieve both spatial and temporal control of multiple-point interactions between

[*] serge.monneret@fresnel.fr; phone 33491288052; fax 33491288063; http://www.fresnel.fr/mosaic/

beads and cells. As a result, we have developed a complete system based on holographic optical tweezers to locally apply several beads on target cells. We then have the possibility to define specific two- or three-dimensional beads patterns according to the target cell shape, and perform a sequential manipulation of individual beads.

Finally, as we plan to use our system to study biological events in the one hour timescale, we have to keep beads and cells separated, in order to prevent unwanted beads to move freely in the sample and interact with the target cell during the experiment. Hence, to keep target cells and handles separated, we devised custom microchambers which comprise fluidic reservoirs that are typically 100-1000 µm big in diameter, in order to facilitate their manual filling. Such values are significantly high to prevent the microfabrication of complete monolithic chips with conventional lithography-based microfabrication processes. We then introduce micro-stereolithography as a 3D micro-manufacturing approach for the rapid prototyping of microchambers comprising wells to locally inject beads inside the sample and keep them separated from cells in our essays.

Some previous works combining optical tweezers and microfluidics have already been presented. Optical tweezers have been used as a tool to ensure continuous isolation of single bacteria cells in 5 µm high microchambers by removing out excess cells in order to realize on-chip single-cell microcultivation [10-11]. In another experiment, microspheres have been transferred into the input port and directed to one of the two output ports of a T-channel, by using the trapping force of an optical tweezers to drag and release the objects within the laminar flow stream [12]. Bacteria cells have also been moved from one reservoir to another without the media being dragged along with them by means of dual optical tweezers on a timescale of few seconds [13]. Recently, multiple bacteria have been manipulated inside a 200 µm thick simple microchannel thanks to holographic optical tweezers [14].

In this paper, we combine holographic multiple optical tweezers with a microfluidic system to create a versatile microlaboratory. We first present our holographic optical tweezers setup, and a convenient way to address several planes simultaneously. We also present the combination of HOT with a supplementary fully steerable manual optical tweezers facility. We then demonstrate the possibility for microSL to easily and rapidly fabricate small three-dimensional observation chambers with customized design of the flow channels and, finally, we demonstrate the combination of HOT with microSL to apply multiple beads on target cells, the excess beads being kept enclosed inside a three-dimensional reservoir. Please note that in this paper, all trapped particles in the experiments are silica 2µm-diameter beads.

2. MULTI-PLANES HOLOGRAPHIC OPTICAL TWEEZERS

2.1. Holographic optical tweezers

Holographic optical tweezers (HOT) allow the trapping beam to be split up into more than one trap at different positions, by means of a diffractive optical element (DOE) which is generally a hologram. Most holographic setups place the traps in the Fourier-plane of the DOE implying that a linear phase at the DOE results in a lateral displacement of the optical trap. Originally demonstrated with a commercial diffractive 4x4 square array generator [15], HOT have since then been implemented with a computer-addressed spatial light modulator as the DOE, allowing diffractive pattern to be quickly replaced in a cartoon fashion, and dynamically reconfigure the resulting spatial distribution of traps [16, 17].

HOT use holograms that are almost always phase holograms, also called kinoforms, as intensity holograms would decrease the power in the trapping beam. Moreover, diffractive elements which solely rely on a phase modulation of the incident beam lead, in ideal conditions, to a single reconstruction order without the annoying and power disturbing presence of the zero order [18]. But, as with gratings, limitations in phase linearity and in the spatial resolution of the DOE result in some of the light remaining in the zero order or being diffracted into higher orders which may create unwanted traps.

2.2. HOT setup

Figure 1 shows our version of holographic optical tweezers. It has been built by modifying an inverted microscope so that a laser beam can be introduced into the optical path right before the objective. This is achieved by means of a

dichroic mirror (R > 99% @1050 nm, T > 80% @ 400-700 nm, CVI, New Mexico, USA) which does not compromise the original conventional imaging and fluorescence imaging capabilities of the microscope. Therefore, it is possible to record fluorescence emitted by cells submitted to trapped beads contacts.

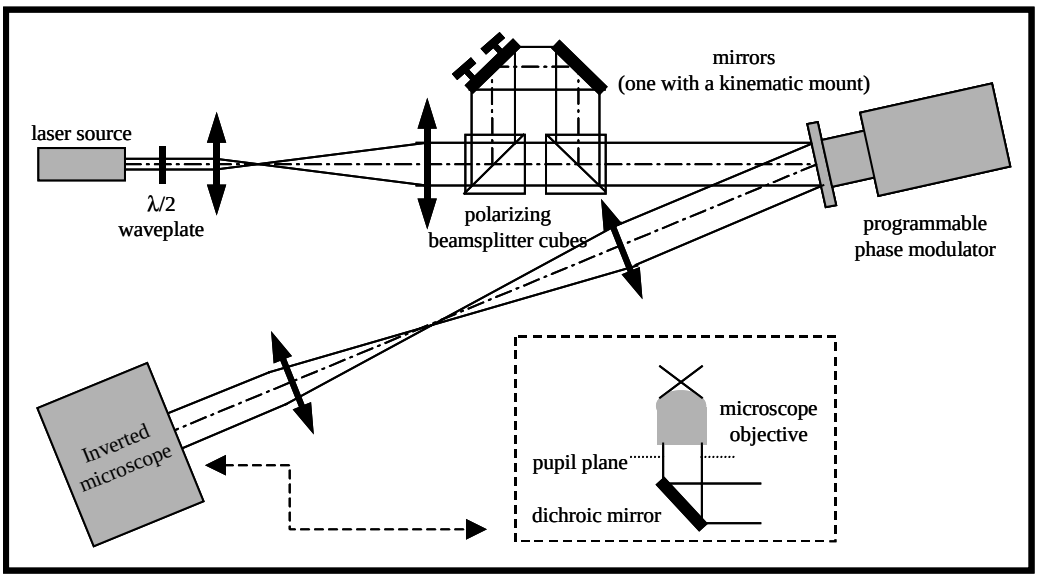

Figure 1: Scheme of the HOT setup

The holographic optical bench is built around an Hamamatsu X8267 programmable phase modulator (PPM). The PPM is an optically addressed nematic-liquid-crystal device, configured to act as a phase hologram that uses 256 phase levels. It has a 768x768 pixels resolution without sharp pixelation, suppressing the loss of power into additional, widely-spaced diffraction orders [19]. As a result, typically over 80% of the incident light is diffracted into the optical traps. The laser linearly polarised beam comes from a near infrared 2W fibre laser source (IPG Laser, Germany); it is collimated by a first ×4 telescope to fit the PPM active surface, and finally resized from a second × 0.83 telescope to fill up the entrance pupil of a 40×, NA = 1.3 oil immersion objective (5 mm focal length). We use the PPM at an angle of incidence of 4.5°. The second telescope is also defined for the DOE plane and the entrance pupil of the microscope objective to be optically conjugated. As a consequence, a beam of light passing through the DOE also passes through the pupil, minimizing power losses with diffraction angle.
The incorporation of two 25mm travel range, 2µm resolution, crossed-roller bearing linear translation stages (Physik Instrumente, Germany) affords dynamic positioning of the sample chamber relative to the traps, and greatly facilitates calibration. They also permit traps to make programmed travels (velocity, acceleration, displacement, position memory) between millimetric reservoirs and target cells. Moreover, the objective can be axially displaced by a PIFOC piezoelectric system capable of 10 nm resolution (PIFOC, Physik Instrumente, Germany).

Figure 1 also shows a λ/2 waveplate and two polarizing beam splitters which are used to create a very useful single, manually steerable trap (one of the two mirrors is fixed on a kinematic mount). A detailed description of the system and its interest for sequentially applying beads on cells are given in section 3.

2.3. 2D parallel manipulation of particles

Creation of separate traps is achieved by diffracting a single collimated laser beam into a desired distribution of beams, from a specific complicated phase pattern DOE. Thus, the definition of the DOE, with respect to the diffraction efficiency, zero and high orders diffraction residuals, and computation time, is the key to holographic trapping.
Obtaining a desired wavefront in the focal plane of the microscope objective requires generating the appropriate wavefront in the DOE plane. Because optical trapping solely rely on the beam's intensity and not on its phase, we are able, by just modifying the phase of the incoming (generally gaussian) laser beam at the DOE plane, to obtain the desired trapping configuration [15]. Moreover, phase-only holograms optimise the power losses during the diffraction step.

The calculation of phase holograms needed to project a desired pattern of traps at the sample plane is not straightforward. The first computer-generated holograms were calculated from analytical phase distribution similar to that of a TEM_{01} mode; then holograms were superimposed to generate multiple independent traps [16]. This method was computationally very fast but also created unwanted ghost traps. An iterative numerical technique based on an adaptive-additive algorithm has then been used to generate arrays of identical tweezers from binary phase holograms [15], but again suffered from ghost traps. Finally, following the approach pioneered by Gerchberg and Saxton (GS) [20], it was possible to iteratively calculate DOE by means of a generalized Fourier transform, allowing to transform given conventional traps into another type of trap like an optical vortex [21] and, at the same time reduce the problem of ghost traps.

In our case, we also used a Fourier-transform-based Gerchberg-Saxton algorithm slightly modified in order to control the computation time rather than the reconstruction error. This is a fundamental requirement to assure a fixed rate of kinoforms calculation for real-time essays. However, a little tuning on the algorithm parameters, such as error-reduction equation coefficients and initialisation, is necessary for this approach to provide satisfying result.

Figure 2 gives examples of a 2D light patterns of free traps, demonstrating the absence of high diffraction orders, and also the possibility to strongly decrease the zero order intensity. Figure 3 demonstrates the application in dynamic optical tweezers. It shows an example of trapping and rearrangement of eleven 2 µm-diameter silica beads; a sequence of 46 hologram patterns was pre-calculated and then displayed on the PPM over a period of 11s.

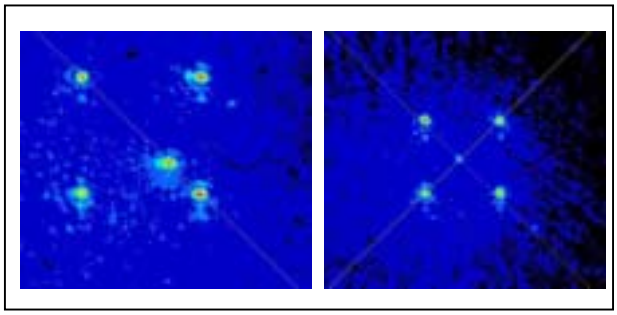

Figure 2: 2D non centered square pattern of free traps demonstrating the absence of high diffraction order (left), and symmetric pattern with also reduced zero order (right).

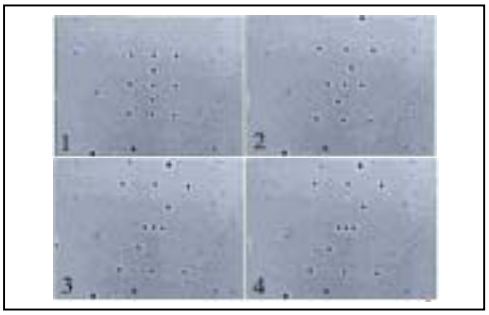

Figure 3: 2D dynamic trapping sequence of 11 silica beads of diameter 2µm, realized by means of 46 pre-calculated holograms.

2.4. 3D manipulation of particles

The ability to introduce focal power with the PPM means that the traps can be manipulated axially allowing controlled 3D positioning within the sample cell volume, typically over a range of several 10's of micrometers. Complex three-dimensional structures have been assembled and manipulated in this way [22, 23, 14]. Control over 3D trapping positions in HOTs was first achieved by adding lens holograms to the individual trap holograms (simple blazed gratings) before superimposing [19, 24]. Direct binary search algorithms have also been proposed to calculate a series of hologram patterns, which have been successfully displayed on a spatial light modulator to dynamically trap 4 beads with a 3D distribution in the sample volume [24]. At last, a specific multi-plane Gerchberg-Saxton algorithm has been developed for 3D light shaping [25], and compared to direct binary search (DBS) algorithms [**Erreur ! Source du renvoi introuvable.**]. As a result, DBS algorithm is slower than the GS one, preventing it from being used interactively. However, the DBS algorithm allows control of the intensity in an arbitrary number of planes, where GS algorithm slows as soon as the number of planes increases [22].

We here propose Quadrant Kinoform (QK) as a novel approach to obtain three-dimensional trapping pattern at reasonable resolutions, allowing interactive dynamic 3D manipulation of particles. QK is based on the well-known hologram property to reconstruct the virtual object even when the hologram is broken; as a matter of fact, each part of the hologram contains the information about the whole object from different spatial points of view. The SLM addressable area is multiplexed into smaller logical units with lower reconstruction efficiency, due to the reduced kinoform size, which are then addressed with a peculiar trap pattern independently. Moreover, to achieve the three-

dimensionality of the whole pattern, each unit is projected at different focus depth through the addition of a coaxial lens term (figure 4) calculated on the base of the following mathematical expression :

$\Phi_{lens}(x,y) = \frac{2\pi n_{med}(x^2+y^2)\,z}{f_{obj}^2\,\lambda}$, where n_{med} is the medium index, λ the laser wavelength, x, y the coordinates being the center of the DOE the origin, f_{obj} the objective focal length and z the desired focal shift.

In such a way, a three-dimensional arrangement of traps can be achieved (figure 5), the number of units being the addressable planes. It is important to underline the independency and versatility of each unit: if the pattern on a specific plane has to be rearranged, it can be done by simply recalculating the corresponding DOE shown on the unit preserving the others, thus boosting the time required for small modifications. In the same way, changing the depth of a plane is easily accomplished recalculating the lens term and not the whole hologram. Another advantage is the easy power management. Balancing the power among planes is reduced to a mere unit resizing or re-centering of the incident beam on the DOE, having in mind that there is a lower limit in the kinoform size below which a reconstruction is no more resolved enough to be useful.

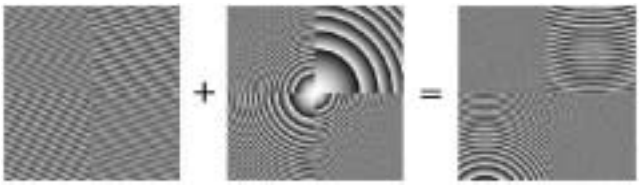

Figure 4: Basic principle of Quadrant Kinoform. An hologram composed of four different subunits is combined with four lens terms to obtain a three-dimensional reconstruction onto 4 different planes.

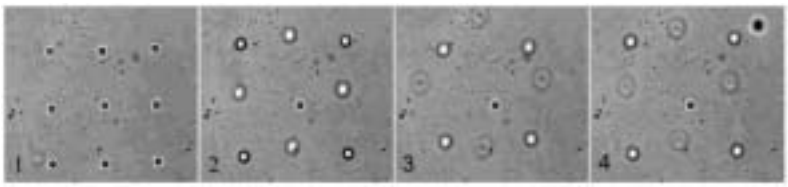

Figure 5: Use of quadrant kinoform to trap nine 2 µm silica beads
which move from a common plane to two new ones and describe a peristaltic movement.

3. COMBINING HOT AND SINGLE MANUALLY STEERABLE OPTICAL TWEEZERS

3.1. Setup

Let us come back on the manually steerable single optical tweezers (SOT) described previously (figure 1). In the phase modulation mode, the liquid crystal molecular axis of the PPM should be set parallel to the polarisation direction of the incident beam laser for diffraction to occur. As a consequence, light beam coming from the manually steerable optical path is linearly polarised, with a polarisation state orthogonal to the liquid crystal molecular axis (figure 6); thus it does not diffract on the PPM, which only acts as a mirror. Moreover, placing a $\lambda/2$ waveplate before the polarizing beamsplitter cubes (figure 1) permits to adjust the power ratio between the manually steerable trap and the set of holographic ones. As a result, it is possible to realize relatively complicated sequences, by playing with both the power ratio and the single/multiple nature of optical tweezers.

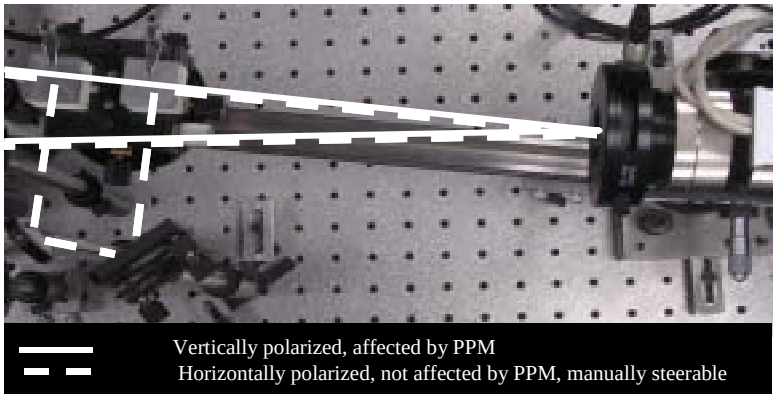

Figure 6: Picture of the manually steerable optical tweezer.

3.2. Sequential deposition of beads on a target cell

Combination of HOT and manually steerable independent SOT affords to fully control the sequential deposition of beads on a target cell. Indeed, HOT allow to maintain a given number of beads with a specific pattern trapped in the vicinity of the cell, thus creating like a small temporary beads reservoir close to it. Then, modifying the power ratio between HOT and SOT, combined with changes in the HOT trapping plane, permits to transfer a bead from a HOT trap to the SOT one, and finally to make it travel to a given position on the target cell. Figure 7 gives a schematic view of the procedure, which has been used experimentally (see section 5.3).

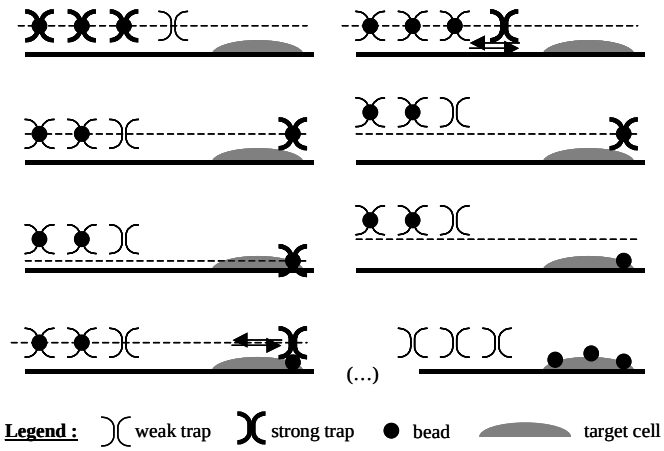

Figure 7: Procedure description to sequentially deposit beads on a target cell. Temporary local beads reservoir is provided by HOT.

4. MICROSTEREOLITHOGRAPHY

Stereolithography (SL) corresponds to a layered manufacturing methodology in which objects are built as a stack of horizontal cross sections, each one being formed individually by a light-induced photopolymerisation chemical reaction [26]. Thin layers of liquid material are thus sequentially solidified and stacked from bottom to top to create complicated three dimensional structures. Micro-SL [27] is now one of the most promising manufacturing processes for polymer microparts with complex shapes [28], which has also been used to realise ceramic micro-components [29]. Another advantage is that it may be used without the need for a cleanroom facility.

Figure 8 shows the system we developed, which integrates as major sub-systems an ultra-violet (UV) lamp coupled with a flexible light guide, a dynamic mask, a projection/reduction lens, a motorized translation stage, a motorized scraper and a personal computer.
The UV light beam comes from a 200 W high pressure mercury-xenon lamp (LC5 system, Hamamatsu, Japan). Since the uniformity of the light illumination is a critical factor that determines the process reliability, a specific lens (fly-eye type, Hamamatsu, Japan) has to be introduced at the lamp flexible light guide output, providing a uniform illumination on the mask.

The dynamic binary mask is the core component of the system as it determines the shape of the fabricated micropart. It is composed of a digital micromirror device (DMD), which was part of a Texas Instrument Digital Light Processing Discovery 1000 Starter Kit (Texas Instruments, Dallas, TX, USA), designed for optical use in the UV range. The Controller Board uses the Texas Instruments DMD 0.7 XGA DDR device, which is a spatial light modulator that consists of a 1024 x 768 array of aluminium micro-mechanical mirrors with a 13.7-micrometer pitch and a 85% optical fill factor. Each mirror can be individually deflected with two stable resting states tilted ±12° to the surface normal, about a hinged diagonal axis. Deflection angles (positive or negative) of the mirrors are individually controlled by changing the address voltage of underlying CMOS addressing circuitry and mirror reset signals [30].
The device acts as a reflection-type spatial light modulator. When the mirrors are set at +12°, light originating from the uniform illumination lens is directed towards the photographic lens. On the other hand, when they are set at –12°, light is deflected out of the imaging system. Moreover, the contrast ratio of the dynamic mask is sufficient to use it also as a shutter.

Photographic lenses (50 mm focal length, F/1.2) allow to image the dynamic binary mask onto the surface of the photocurable resin, with a variable magnification in order to control the size of the object. The vertical motorized translation stage moving the support gives the nominal value of the layer thickness. A DC driven micrometer fitted with a magnetic encoder is used to verify position, with an accuracy of 2 µm. The speed, acceleration and distance of travel are programmed independently. The scraper, a metallic blade, performs regular back and forth motions at the free surface level.
The personal computer is used to control the support and scraper motions, and provides the input for the dynamic mask.

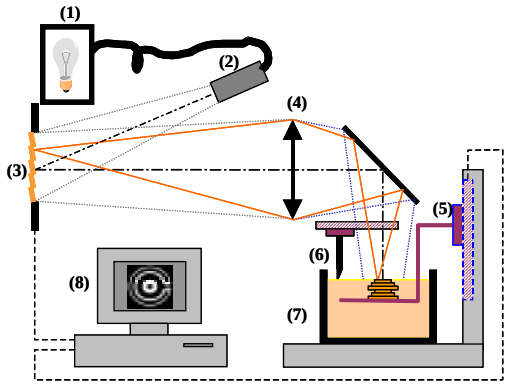

Figure 8: Scheme of the microstereolithography setup
(1) high pressure Hg light source ; (2) dynamic mask (DMD) ; (3) uniform illumination lens ; (4) projection/reduction lens ; (5) vertical moving stage ; (6) scraper ; (7) bath of liquid resin ; (8) personal computer.

The principle of layer stacking used during the microfabrication process is as follows (figures 8 and 9): a metallic plate supporting the object to be manufactured is positioned at a small distance below the surface of the liquid. The modulated light beam coming from the dynamic mask is transferred through the reduction lens, and an image is focused at the free surface of the liquid resin with a reduced feature size. This image defines a 2D binary pattern, which induces a polymerisation reaction in the illuminated areas solidifying the resin there, while in the dark regions it remains liquid (step 1, figure 9). After the first layer is polymerised, the support sinks down one layer thickness in the resin. A scraper then applies new fresh material on top of the existing structure and makes the free surface uniform (step 2, figure 9).

Because of the weak layer thickness (20-50 µm typically), supplementary relaxation time is necessary to ensure the surface to be uniform (step 3, figure 9). Finally, a new pattern is displayed on the mask, and so on, following the shape of the object, which thus sinks stepwise in the resin bath as new solid layers are formed.
Once fabricated, the object is moved out of the bath and washed with a solvent. The adhesion on the metallic support is weak enough to prevent any damage when the solid micropart is taken off.

According to the third step of the deposition process (figure 9), the photocurable material must have a viscosity as low as possible. Indeed, the relaxation time depends mainly on the rheological properties of the resin. The curable system used in this paper consists of 1% photoinitiator (Irgacure 819, Ciba Specialty Chemicals) dissolved in a photocurable mixing of monomers, composed of 70% with pentaerythritol triacrylate (PETIA, UCB Chemicals) and 30% with 1,6-hexanediol diacrylate (HDDA, UCB Chemicals). With such a material, the fabrication rate is of 2 layers per minute, with an exposure time of 800 ms for 50 µm thick layers.

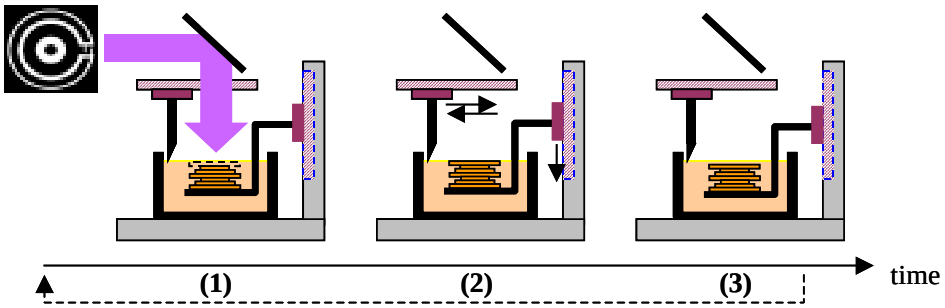

Figure 9: Main steps of the fabrication process. (1) Pattern-shaped photocuring ;
(2) Deposition of a new layer of liquid material ; (3) Relaxing the new layer of fresh resin

As for the conventional SL technique, the microfabricator can just be considered as a sophisticated output device for computers. The object to be built is generally designed with Computer Aided Design tools like solid 3D modellers; then data transfer is made using the binary STL encoding, which is the standard data transfer format for additive fabricators like SL devices. In this way, surfaces of the product are approximated with triangles facets whose vertices are ordered to indicate which side of the triangle contains the mass. The accuracy of a non-planar surface then strongly depends on the number of facets used to approximate the surface.

The STL file is only a faceted representation of the exterior surfaces of the object. In order to build the part, its 3-D shape is then broken down into a sequence of cross sections, like contours on a topographic map. This means that the object is mathematically sectioned by a slicing algorithm into a series of horizontal planes. After that, a special program defines a complete set of binary masks corresponding to the different cross sections. In the following step, the masks are sequentially sent to the automated machine, in order to build the object. Fig. 10 gives the three main steps of the global microfabrication process, from the CAD file to the image of the obtained three dimensional micro-object. The design-to-fabrication time is typically one hour for fabricating 10mm of height microchambers.

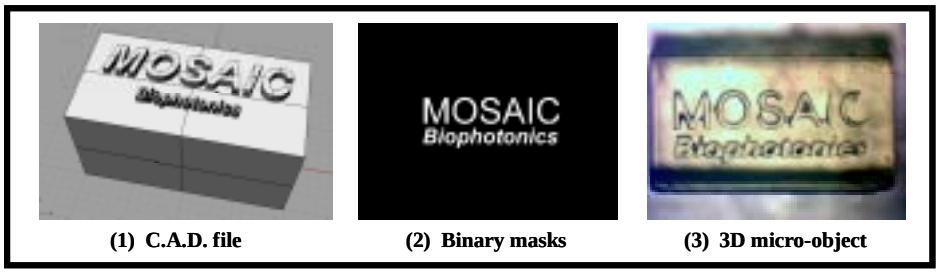

Figure 10: The three main steps of the global microfabrication process

Three-dimensional structures containing reservoirs, outlets, and walls with different shapes have been fabricated with microSL (figure 11). Varying the layer thickness during the fabrication is possible and advised as it allows to optimize the fabrication time by increasing the thickness when simple and regular structures are being built, and decreasing it when details are needed (this can be easily seen in figure 11, reservoirs 2 and 3). Because of the relative big size of the reservoirs, the layer thickness was ranging between 50 and 100 µm, allowing them to be made in less than one hour.

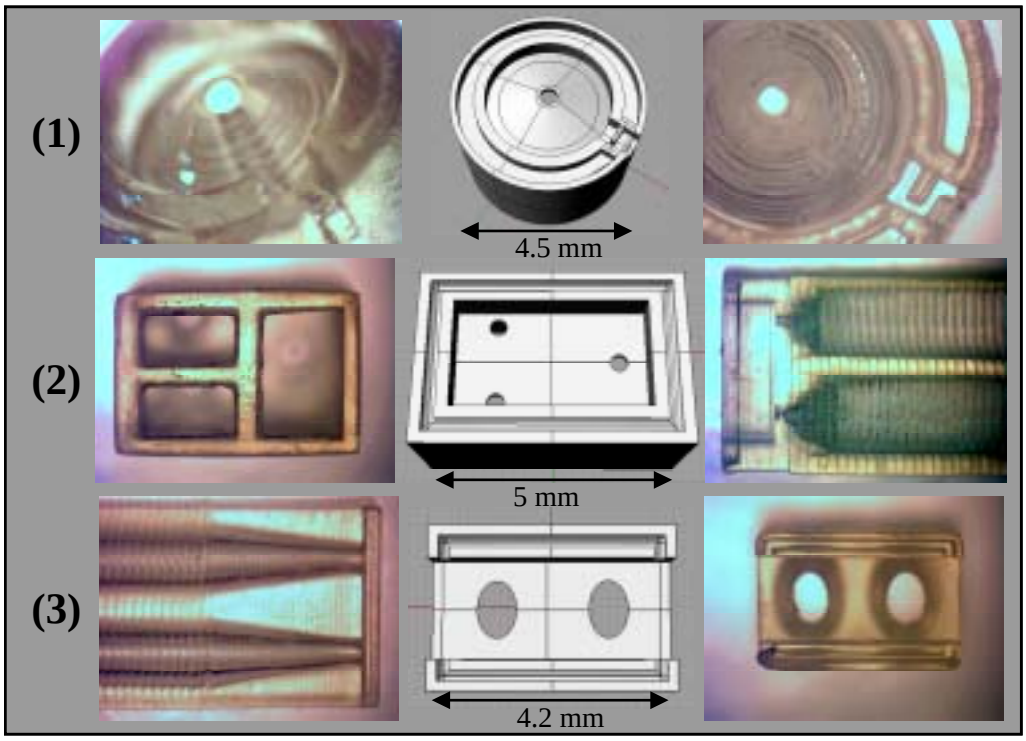

Figure 11: Examples of 3D structures containing reservoirs

5. PRACTICAL LAB FOR THE SPATIO-TEMPORAL CONTROL OF BEADS/CELL INTERACTION

5.1. Microfabrication of a specific reservoir for maintaining beads in a restricted area in a liquid sample

A specific reservoir structure has been realized in order to keep beads and cells separated in a liquid sample, and hence to allow the control of beads/cell interaction. This reservoir was composed of 75 layers, each one of 100 µm thickness (figure 12-1). Once fabricated, the reservoir was bounded to a manually-driven X-Y-Z translation system and then applied on a commercially available chambered coverglass (figure 12). A buffer solution has then been introduced into the entire microfluidic system to prevent bubbles formation; then we injected inside the reservoir a few µl of a new buffer-based solution containing the beads, by means of a manual syringe. Shortly after, beads started sinking with gravity and then remained confined on the glass substrate in the "confinement chamber" (figure 12-2). Figure 13 demonstrates a relatively precise position of the beads under the reservoir outlet (figure 13), showing that polymeric structures allow to confine beads in a restricted area in liquid macroscopic sample. We then were able to combine this technique with HOT for controlling beads/cell interactions.

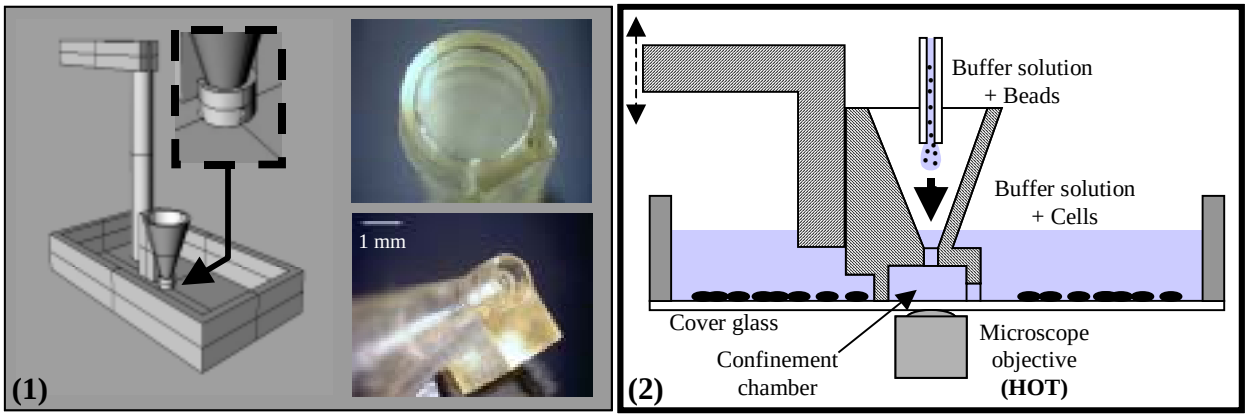

Figure 12: A specific reservoir structure to keep beads and cells separated in a liquid sample composed of 75 layers, each one of thickness 100 µm (1). Once fabricated, the reservoir is bounded to a manually-driven X-Y-Z translation system and then applied on a commercially available chambered coverglass (2).

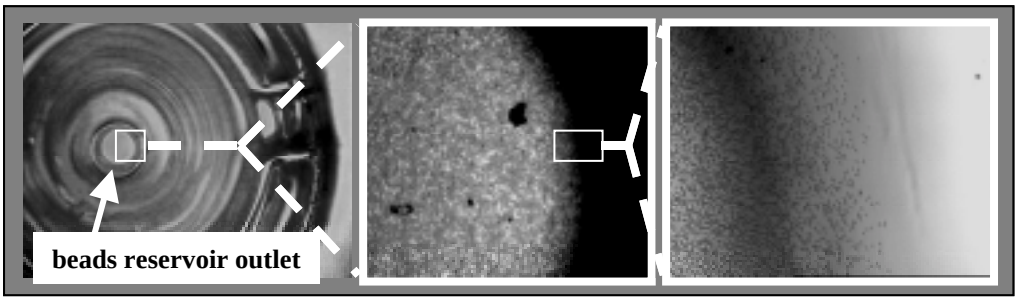

Figure 13: Beads dispersion on the microscope cover glass placed under the reservoir outlet. One can confirm the limited diffusion of beads on the glass, and hence demonstrate the ability of the polymeric structure to confine them in a restricted area.

5.2. Place an array of beads above a cell with a given 2D pattern and adjust its size in real time

The reservoir was applied on a chambered coverglass, which contained cultivated cells, as shown in figure 12-2. One of the cells was chosen to be the target, and its position was recorded as a refeference. Then silica beads were injected inside the structure. Three of them were trapped while sinking by means of HOT, and were moved outside the confinement chamber, up to the referenced target cell (figure 14). Relative adjustments on the global positioning of the beads pattern above the target, but also on its scale were made in real time, by using the sample positioning system and by modifying the zoom factor of the displayed kinoform on the PPM. Afterwards, the beads were put into contact with the target cell, by moving the sample in the axial direction.

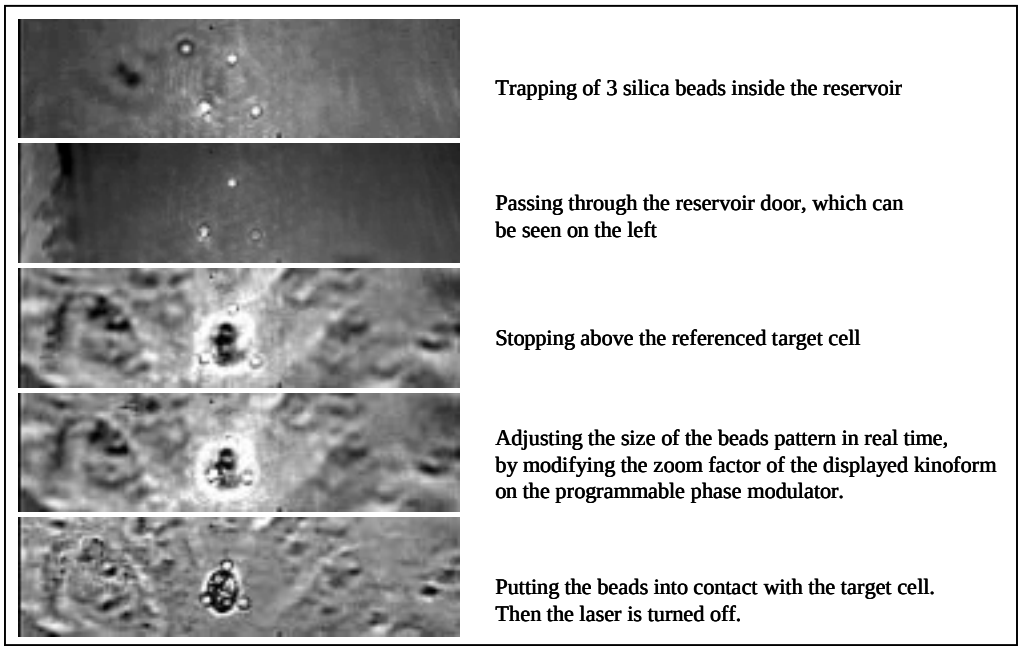

Figure 14: Parallel and simultaneous contact between 3 silica beads and one target cell

5.3. Parallel transport of beads on a target, and control of the temporal distribution of contacts on it

As seen before, HOT can be used to create temporal beads "reservoirs" close to a target cell, as described on figure 7. Figure 15 shows an axample of beads deposition on a target, using combination of HOT and SOT, with changes in the HOT trapping plane by means of real-time displayed Fresnel lenses on the kinoform. Four silica beads were trapped inside the polymeric confinement chamber, and moved close to the target. SOT laser power was then increased to be greater than that of the HOT, in order to permit us to sequentially extract beads from the HOT traps, and to manually drive them up to the target, as described in the figure 7.

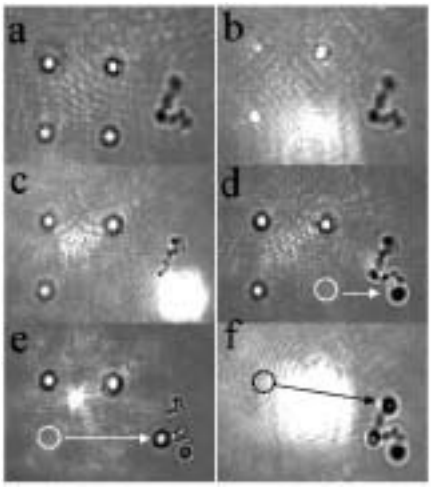

Figure 15: Sequential real-time deposition of 3 silica beads on one target

6. CONCLUSION

In this paper, we demonstrated that we are now able to present multiple beads to well-defined regions of individual target cells. Both sequentially and parallel deposition of beads are possible, with a spatio-temporal control of the deposition procedure. Our approach based on holographic optical tweezers is ideal for investigating multiple simultaneous ligand-based cellular interactions, because of the easily user-defined contact geometry, timing, and ligand nature (not presented in this paper). Moreover, we are able to observe the cell before, during and after activation without being disturbed by free travelling beads inside the sample, because we are able to keep the beads inside confinement chambers. Beads injection into such chambers is easily accomplished because the confinement zone is placed under three-dimensional reservoirs allowing a manual filling with conventional syringes. Our apparatus will be applied very soon to the study of cellular activation patterns. In particular, we plan to measure the effect of costimulation on the activation of phagocytosis in macrophage cells, by presenting multiple antigen-coated beads at varying surface densities to well-defined regions of individual target cells.

ACKNOWLEDGMENTS

This work has been supported in part by CARL ZEISS S.A. and the "Conseil Régional de la Région Provence-Alpes-Côte d'Azur". HOT set-up has been supported by the CEE. Microstereolithography has been supported by the CNRS-MRCT. The authors would like to thank Olivier Soppera from the "Département de Photochimie Générale" (Mulhouse, France) for developing the microSL material.

REFERENCES

1. S. Heidemann, D. Wirtz, "Towards a regional approach to cell mechanics", Trends in Cell Biology 14, 160-166 (2004).
2. A. Ashkin, J. Dziedzic, J. Bjorkholm, S. Chu, "Observations of a single-beam gradient force optical trap for dielectric particles", Opt. Lett. 11, 288-290 (1986).
3. K. Neuman, S. Block, "Optical trapping", Review of Scientific Instruments 75, 2787-2809 (2004).
4. D. Raucher, M. Sheetz, "Characteristics of a membrane reservoir buffering membrane tension", Biophys. J. 77, 1992-2002 (1999).
5. C. Galbraith, M. Sheetz, "Keratocytes pull with similar forces on their dorsal and ventral surfaces", J. Cell Biol. 147, 1313-1323 (1999).
6. D. Raucher, M. Sheetz, "Cell spreading and lamellipodial extension rate is regulated by membrane tension", J. Cell Biol. 148, 127-136 (2000).
7. W. Huang, B. Anvari, J. Torres, R. LeBaron, K. Athanasiou, " Temporal effects of cell adhesion on mechanical characteristics of the single chondrocyte", Journal of Orthopaedic Research 21, 88–95 (2003).
8. X. Wie, B. Tromberg, M. Cahalan, "Mapping the sensitivity of T cells with an optical trap: polarity and minimal number of receptors for Ca^{2+} signaling", PNAS 96, 8471-8476 (1999).
9. A. Caspi, O. Yeger, I. Grosheva, A. Bershadsky, M. Elbaum, "A new dimension in retrograde flow: centripetal movement of engulfed particles", Biophys. J. 81, 1990-2000 (2001).
10. Y. Wakamoto, S. Umehara, K. Matsumura, I. Inoue, K. Yasuda, "Development of non-destructive, non-contact single-cell based differential cell assay using on-chip microcultivation and optical tweezers", Sensors and Actuators B 96, 693-700 (2003).
11. S. Umehara, Y. Wakamoto, I. Inoue, K. Yasuda, "On-chip single-cell microcultivation assay for monitoring environmental effects on isolated cells", Biochem. Biophys. Res. Comm. 305, 534-540 (2003).
12. M. Ozkan, M. Wang, C. Ozkan, R. Flynn, A. Birkbeck, S. Esener, "Optical manipulation of objects and biological cells in microfluidic devices", Biomed. Microdevices 5, 61-67 (2003).
13. J. Enger, M. Goksör, K. Ramser, P. Hagberg, D. Hanstorp, "Optical tweezers applied to a microfluidics system", Lab Chip 4, 196-200 (2004).
14. E. Ferrari, V. Emiliani, D. Cojoc, V. Garbin, M. Zahid, C. Durieux, M. Coppey-Moisan, E. Di Fabrizio, "Biological samples micro-manipulation by means of optical tweezers", Microelectronic Engineering 78-79, 575-581 (2005).

15. E Dufresne, D G Grier, “Optical tweezer arrays and optical substrates created with diffractive optics”, Rev. Sci. Instr. 69, 1974-1977 (1998).
16. M. Reicherter, T. Haist, E. Wagemann, H. Tiziani, "Optical particle trapping with computer-generated holograms written on a liquid-crystal dysplay", Opt. Lett. 24, 608-610 (1999).
17. P. Mogensen, J. Glückstad, "Phase-only optical encryption", Opt. Lett. 25, 566-568 (2000).
18. L B Lesem, P M Hirsch, J A Jordan, “The kinoform: a new wavefront reconstruction device”, IBM Journal of Research and Development 13, 150-155 (1969).
19. J Liesener, M Reicherter, T Haist, H J Tiziani, “Multi-functional optical tweezers using computer-generated holograms”, Opt. Comm. 185, 77-82 (2000).
20. R. Gerchberg, W Saxton, "A practical algorithm for the determination of the phase from image and diffraction plane pictures" Optik **35,** 237-46 (1972).
21. J E Curtis, B A Koss, D G Grier, “Dynamic holographic optical tweezers”, Opt. Comm. 207, 169-175 (2002)
22. G. Sinclair, P. Jordan, J. Courtial, M. Padgett, J. Cooper, Z. Laczik, "Assembly of 3-dimensional structures using programmable holographic optical tweezers", Optics Express 12, 5475-5480 (2004).
23. D Cojoc, V Emiliani, E Ferrari, R Malureanu, S Cabrini, R Z Proietti and E Di Fabrizio, “Multiple Optical Trapping by Means of Diffractive Optical Elements”, Jap. Jour. Appl. Phys. 43, 3910-3915 (2004).
24. J. Leach, G. Sinclair, P. Jordan, J. Courtial, M. Padgett, "3D manipulation of particles into crystal structures using holographic optical tweezers", Optics Express 12, 220-226 (2004).
25. G. Sinclair, J. Leach, P. Jordan, G. Gibson, E. Yao, Z. Laczik, M. Padgett, J. Courtial, "Interactive application in holographic optical tweezers of a multi-plane Gerchberg-Saxton algorithm for three-dimensional light shaping", Optics Express 12, 1665-1670 (2004).
26. P. F. Jacobs, Rapid Prototyping and Manufacturing: Fondamentals of Stereolithography, The Society of Manufacturing Engineers, Dearborn, MI (1992).
27. K. Ikuta, K. Hirowatari, "Real three-dimensional microfabrication using stereolithography and metal molding", Proc. of IEEE Micro Electro Mech. Syst., 42-47 (1993).
28. A. Bertsch, S. Jiguet, P. Bernhard, P. Renaud, "Microstereolithography: a review", Mater. Res. Soc. Symp. Proc. 758, LL..1-LL..12 (2003).
29. C. Provin , S. Monneret, H. Le Gall, S. Corbel, "Three-dimensional ceramic microcomponents made using microstereolithography", Advanced Materials 15, 994-997 (2003).
30. see on the web : http://www.tyrexsales.com/dlp/2506197Adisc1100prev.pdf